Corrosion Evaluation of Ferritic Stainless Steels for Automotive Exhaust Applications

Y. Emun,[‡,] H.S. Zurob,[*] and J.R. Kish[*]*

This study compares the localized (exterior) corrosion susceptibility of chromized steel to bench-mark ferritic stainless steels for automotive exhaust applications. Continuous near-neutral salt fog exposure (ASTM B117) was used for this purpose. Corrosion susceptibility was determined using mass loss measurements coupled with a post exposure metallographic examination. Complementary potentiodynamic polarization measurements were made in the bulk salt solution to help interpret the relative performance. The elevated Cr content provided by the chromizing surface treatment provides comparable corrosion resistance to the more highly alloyed ferritic stainless steels studied. The major factor affecting localized corrosion susceptibility is the formation of rust deposits, which act as effective pit-like corrosion initiation sites.

KEY WORDS: atmospheric corrosion, ferritic stainless steel, localized corrosion

Downloaded from http://meridian.allenpress.com/corrosion/article-pdf/75/11/1276/2655949/3319.pdf by guest on 03 October 2024

INTRODUCTION

Increasingly rigorous governmental regulations and passenger expectations have increased demand for longer-life automotive exhaust systems. Current generation systems are typically fabricated using ferritic stainless steels. Ferritic stainless steels provide improved high-temperature oxidation and aqueous corrosion resistance relative to carbon steel variations that were originally used.[1] However, the lower grades of ferritic stainless steel used, such as Type 409 (UNS S40900[(1)]), have become prone to localized corrosion as the service environment has become more aggressive in response to efficiency improvements.[1] Material-based solutions include both aluminized Type 409 stainless steel (Type 409Al), for cold end components, and higher alloyed ferritic stainless steels such as Type 439 (UNS S43035) and Type 436 (UNS S43600), for hot end components:[1] all with an associated cost penalty. Type 409Al involves Cr-lean Type 409 hot-dip coated in Al-10%Si bath creating a galvanically protected stainless steel. Type 409Al is limited to cold end components because of the tendency for intermetallic phase formation in the Al-10%Si coating at temperatures above 600°C.[2]

Chromized steel has been previously considered as an alternative material from which to construct exhaust system components.[3-4] Chromized steel is now once again garnering interest as a candidate material as it offers the combined potential advantage of improved formability (steel substrate) and corrosion resistance (chromized surface) relative to the ferritic stainless steels currently utilized. Of particular interest is the chromized interstitial-free (IF) steel coil product that is produced by Arcanum Alloys. The interest in this material resides in the nature of the chromizing process, which provides a chromized surface treatment to both sides of the IF steel.[5] As this is a new material for exhaust system fabrication consideration, its material performance needs to be well-characterized, including the corrosion resistance (both internal and external) relative to the ferritic stainless steels currently utilized.

The objective of this study is to determine the localized (pitting) corrosion susceptibility of Arcanum Alloy's chromized steel (Optiform[†]) relative to monolithic ferritic stainless steels (Types 409, 409Al, 436, and 439) in atmospheric conditions simulating (external) salt fog/spray exposure. Continuous near-neutral salt fog exposure (ASTM B117) was used for this purpose. Localized corrosion susceptibility was determined using mass loss measurements coupled with a post exposure metallographic examination. Complementary potentiodynamic polarization measurements were made in the bulk salt solution to help interpret the relative performance.

EXPERIMENTAL PROCEDURES

Monolithic ferritic stainless steel sheet metal, including Type 409Al sheet metal, was supplied by AK Steel through Tenneco Automotive (Cambridge, ON). Grades of ferritic stainless steel sheets provided include Type 409 (Fe-11Cr), Type 439 (Fe-17Cr), and Type 436 (Fe-17Cr-1Mo). Chemical compositions obtained by inductively coupled plasma optical emission spectrometry (ICP-OES) were conducted in the MSE department of McMaster University.

The chromized steel sheet metal was supplied by Tenneco Automotive after receiving a production coil from Arcanum Alloys. This steel is comprised of an IF grade steel sheet that was coated with a Cr-rich slurry on one (nonprime) face and then subsequently coiled, heat-treated, and cooled to an ambient temperature. This process produces a chromized surface layer about 80 µm thick on either side of the sheet.[5]

Figure 1 shows an scanning electron microscope (SEM) image of the nonprime (NP) and prime surface (P) layer of the

Submitted for publication: August 8, 2019. Revised and accepted: August 20, 2019. Preprint available online: August 20, 2019, https://doi.org/10.5006/3319. Recipient of first place in the Harvey Herro Applied Corrosion Technology category in the Student Poster Session at CORROSION 2019, March 2019, Nashville, Tennessee.

[‡] Corresponding author. E-mail: yoel.emun@gmail.com.

[*] Centre for Automotive Materials and Corrosion, McMaster University, 1280 Main Street West, Hamilton, Ontario, Canada L8S 4L8.

[(1)] UNS numbers are listed in *Metals and Alloys in the Unified Numbering System*, published by the Society of Automotive Engineers (SAE International) and cosponsored by ASTM International.

[†] Trade name.

ISSN 0010-9312 (print), 1938-159X (online) © 2019 NACE International. Reproduction or redistribution of this article in any form is prohibited without express permission from the publisher.

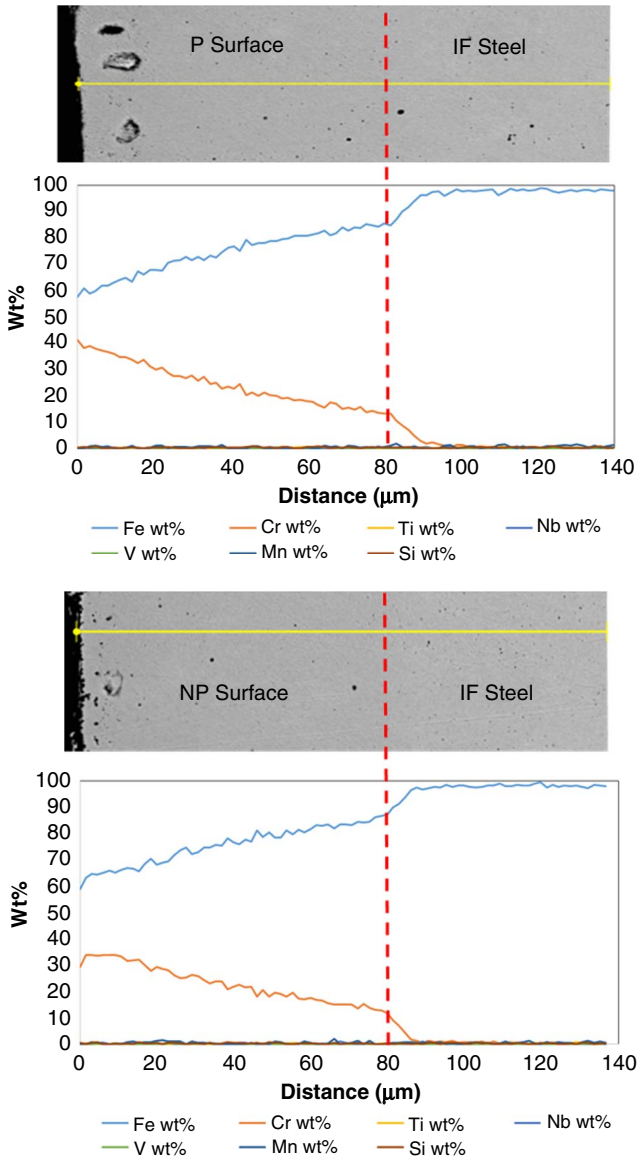

FIGURE 1. *Cross-sectional view of chromized steel sheet metal and associated SEM-EDS line scan results through prime (P) and nonprime (NP) surfaces.*

chromized steel sheet metal in cross section and the associated energy-dispersive x-ray spectroscopy (EDS) line scans across this layer. A well-developed Cr concentration profile is developed at both the nonprime and prime surface. The concentration gradient is nearly linear until about 12 wt% Cr, where there is a significant drop in the Cr content. This drop is consistent with the Fe-Cr phase diagram, which predicts a phase change in the matrix from ferrite (Cr-rich) to austenite (Cr-lean) at high temperatures.[6] The drop effectively demarks the transition from the chromized layer to the IF steel substrate, and is located at a depth of about 80 μm into both surfaces. The Cr content at the surface of the chromized layer is different for the two surfaces: approximately 40 wt% for the prime surface versus 30 wt% for the nonprime surface.

Square (1 cm × 1 cm) samples were prepared from each sheet material to serve as working electrodes for the complementary potentiodynamic polarization measurements. After attaching a Cu wire to the back face using Al tape, samples were cold mounted in epoxy with the RD-TD face boldly exposed to serve as the working surfaces. Preparation for the working surfaces involved ultrasonically cleaning by immersing in reagent grade acetone for 15 min. A conventional three-electrode cell (1,000 mL) coupled with a computer-controlled potentiostat (Gamry Reference 600†) was used to conduct the polarization measurement. Two graphite rods served as the counter electrodes, and an Ag/AgCl electrode served as the reference electrode. The naturally-aerated 5 wt% NaCl(aq) electrolyte, held at 35°C, was made using distilled water and reagent grade NaCl(s). Working electrodes were conditioned at the open-circuit potential (OCP) for 1 h prior to initiating anodic potentiodynamic polarization, starting 300 mV below the OCP. A scan rate of 1 mV/s was used for all measurements and a set of triplicate measurements was made for each sheet metal.

Triplicate sets of rectangular (10 cm × 15 cm) samples were also prepared from each sheet metal, with the long axis made parallel to the rolling direction (RD), to serve as test panels for atmospheric corrosion testing. All panels were ultrasonically cleaned by immersing in reagent grade ethanol for 15 min and weighed to within 0.001 g using a digital balance prior to exposure. All triplicate sets of panels were placed in an Ascott CC450† cyclic corrosion chamber at a 30° angle relative to the normal direction of the chamber. ASTM B117 was the testing protocol used for the salt fog exposure, which consisted of a continuous exposure to a 5 wt% NaCl(aq) salt fog at 35°C.[7] The 1,000 h exposure was interrupted weekly to permit photographic imaging. After completion, panels were removed from the chamber and then photographically imaged, sandblasted to remove corrosion product, reimaged, and finally reweighed to permit a mass loss calculation. Regions of interest were selected for a metallographic examination in cross section. Standard sample mounting and working surface preparation procedures were used to produce a mirror surface finish suitable for examination by light optical microscopy (LOM).

RESULTS AND DISCUSSION

Figure 2 compares a set of typical potentiodynamic polarization curve of each sheet metal recorded in naturally-aerated 5 wt% NaCl(aq) at 35°C. Chromized steel along with Type 436, Type 439, and Type 409 exhibit well-developed passivity that is prone to localized (pitting) corrosion at a distinct breakdown potential. Type 409Al shows active corrosion only, which is consistent with the Al-10%Si surface layer dictating the anodic polarization response. The breakdown (pitting) potentials are listed in the table that is superimposed onto the plot. The prime surface of the chromized steel exhibits the most noble breakdown potential, whereas Type 409 exhibits the least noble one. The trend of increasing breakdown potential mirrors the trend in increasing PRE_N (pitting resistance equivalence number)[8] values, which is listed in the legend for each sheet metal. The higher Cr content of the prime surface layer is responsible for the higher PRE_N relative to the nonprime surface layer. The small difference in breakdown potential between Type 436 and Type 439 is due to the 1 wt% Mo addition, which is a well-established alloying element for increased pitting resistance.[9-10]

Figure 3 shows a set of photographic images of the sheet metals that exhibited visible corrosion after the 1,000 h exposure in the ASTM B117 salt fog test. This set includes Type 409, Type 409Al, and chromized steel. Neither Type 439 nor Type 436 panels showed any visible evidence of corrosion after the 1,000 h of exposure. Corrosion initiated at the cut edges of the

Downloaded from http://meridian.allenpress.com/corrosion/article-pdf/75/11/1276/2655949/3319.pdf by guest on 03 October 2024

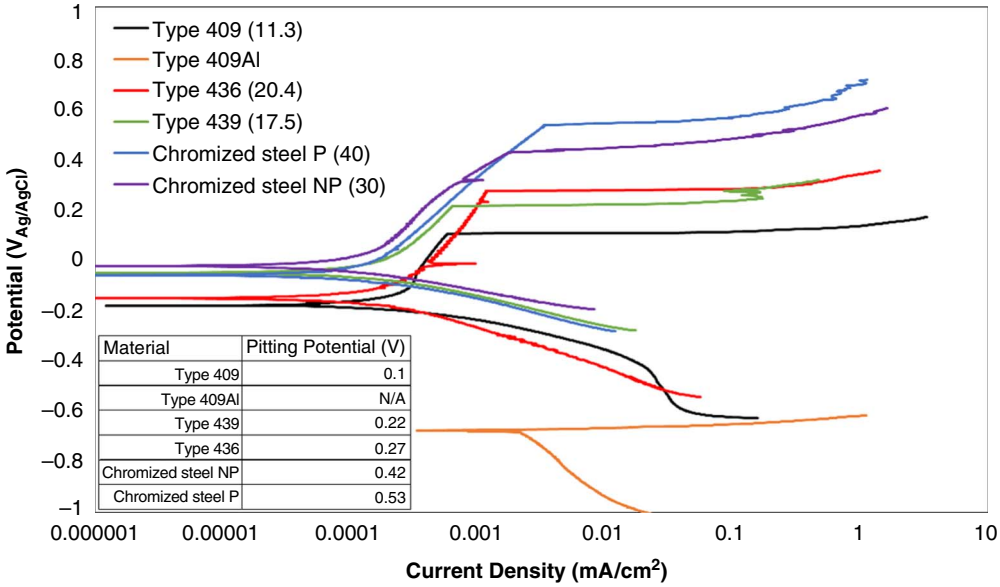

Material	Pitting Potential (V)
Type 409	0.1
Type 409Al	N/A
Type 439	0.22
Type 436	0.27
Chromized steel NP	0.42
Chromized steel P	0.53

FIGURE 2. *Potentiodynamic polarization curves for sheet metals in naturally-aerated 5 wt% NaCl(aq) at 35°C.*

chromized steel panels. The corrosion product (red rust) associated with the top cut edge surface proceeded to migrate down the face surface of the panel. Corrosion of the boldly exposed cut edge was expected as it serves as a galvanic cell comprised of the more-noble Cr-rich surface layer and the more-active IF steel substrate. A similar corrosion appearance was observed on Type 409 panels. The root cause of the increased corrosion susceptibility of the cut edge in Type 409 is currently being investigated.

Figure 3 also shows a photographic image of Type 409Al after 500 h exposure, in addition to one taken after the 1,000 h exposure (Figures 3[c] and [d]). This is necessary to demonstrate the corrosion initially involving the Al-10%Si surface layer, as indicated by the formation of a white corrosion product (presumably $Al(OH)_3$), which then transitioned to red rust formation. This clearly shows that the galvanic corrosion protection of the Type 409 substrate by the Al-10%Si surface layer can be exhausted by accelerated corrosion conditions.

After removal of the corrosion product by sandblasting, an isolated pit-like corrosion indication was found to have initiated underneath the red rust corrosion product present on the face of the chromized steel prime surface. Similar pit-like corrosion indications were observed underneath the red rust corrosion product present on the face surface of the Type 409 panels. The tendency to form pit-like indications underneath rust depots is similar to the tendency of Type 304L (UNS S30403) austenitic stainless steel to do the same as reported by Suleim, et al.[11] They argue that the rust layer deposited onto the stainless steel surface serves as a semipermeable membrane with anion selective properties, lowering the ionic resistance and permitting rapid propagation of localized corrosion.[11] In contrast, the Type 409Al panels exhibited features more consistent with a general corrosion mode than a localized (pit-like) mode, excluding one shallow pit found on the face surface of the Type 409 substrate, after removal of Al-rich corrosion product. Cross sections of pits can be seen in Figure 4.

The mass loss values determined for each sheet metal is compared in Figure 5. The mass loss values have been extrapolated to an annual corrosion rate (mm/y) for ease of interpretation and comparison. Two values are reported for

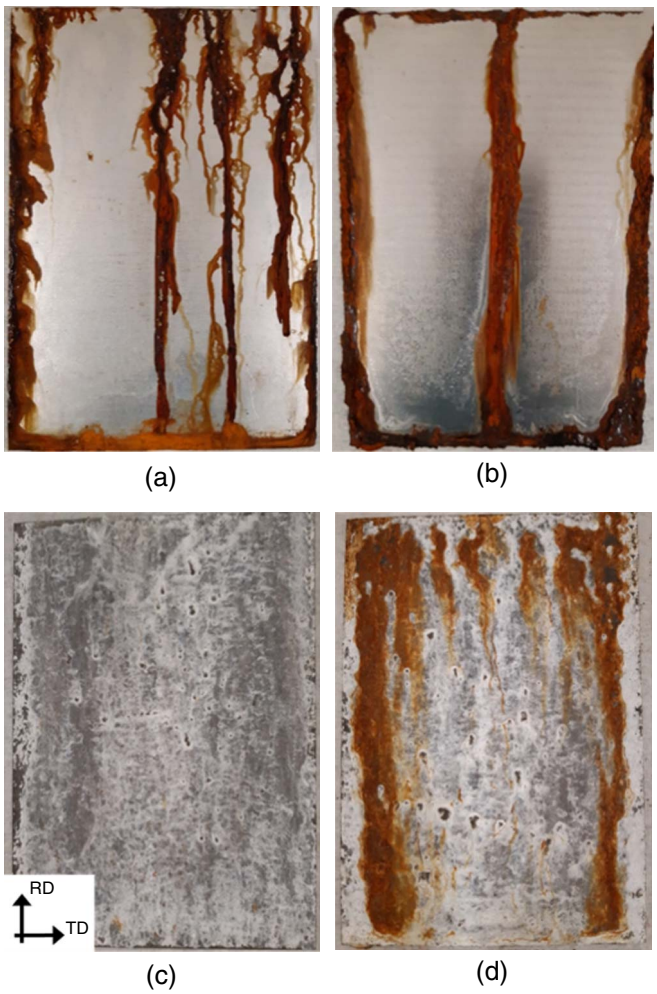

FIGURE 3. *Photographic images of sheet metal panels that exhibited visible evidence of corrosion after 1,000 h exposure in the ASM B117 salt fog test. (a) Type 409 (Fe-11Cr), (b) chromized steel (prime surface), (c) Type 409Al (500 h), and (d) Type 409Al (1,000 h).*

Downloaded from http://meridian.allenpress.com/corrosion/article-pdf/75/11/1276/2655949/3319.pdf by guest on 03 October 2024

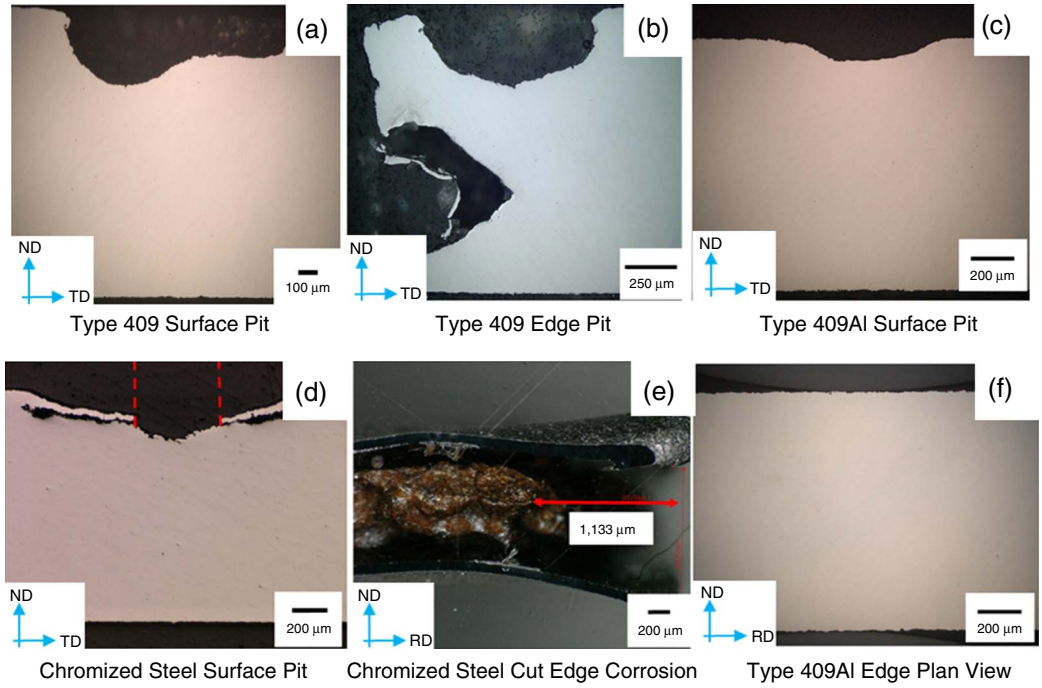

FIGURE 4. *Light optical microscopy images of corrosion indications found after 1,000 h exposure in the ASTM B117 salt fog test.*

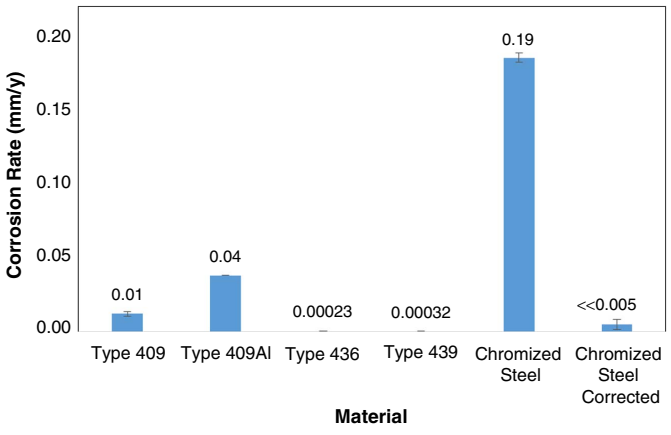

FIGURE 5. *Corrosion rate (mm/y) comparison based on mass loss data after 1,000 h exposure in the ASTM B117 salt fog test.*

chromized steel: an apparent value with the cut edge corrosion included ("Chromized Steel") and a corrected value with the cut edge corrosion excluded ("Chromize Steel Corrected"). The latter was calculated using a first order correction, assuming a consistent thickness of IF steel was lost to corrosion along the entire perimeter of the panel. The IF steel thickness loss was estimated using the photographic image of the cut-edge corrosion (see Figure 4[e]). This method overestimates the corrosion rate, as the depth of corrosion varies along each perimeter, and is most likely much less than the reported 0.005 mm/y. The plot readily shows that the corrected chromized steel yields a corrosion rate that is comparable to Type 436 and Type 439, with the corrosion rate being significantly lower relative to Type 409 and Type 409Al.

The higher corrosion rate exhibited by Type 409Al relative to bare Type 409 is consistent with the consumption of the Al-10%Si surface layer during the 1,000 h exposure and the tendency toward uniform corrosion of Type 409 substrate. It is noted that the aluminized surface layer is applied to provide improved corrosion protection against acid condensate corrosion, which affects the internal surface, not the external surface being considered here.

Figure 4 shows light optical microscopy images of the corrosion indications on the various sheet metal panels in cross section. The pit-like indication on chromized steel (Figure 4[d]) shows the indication propagated through the chromized layer and into the IF steel substrate. Interestingly, once through the chromized layer, the corrosion proceeded laterally along the chromized layer/IF steel substrate interface to a much greater extent than into the IF steel substrate. This feature is consistent with galvanic corrosion involving the more-noble chromized surface layer and the more-active IF steel substrate. The cut edge corrosion was significantly more severe, reaching a depth of about 1,100 µm in the IF steel substrate (Figure 4[e]). A consistent depth of attack was observed on all four exposed cut edges. The greater extent is consistent with corrosion initiating on the cut edge of chromized steel. The pit-like indications formed underneath the rust deposits found on Type 409 were significantly deeper than that formed on Type 409Al. This difference is consistent with the Type 409Al substrate being galvanically protected by the Al-10%Si surface layer during the initial exposure (at least up to 500 h). A plan view image of the Type 409Al cut edge showed no remnants of the Al-10%Si surface layer intact on the Type 409 substrate. A cross section through the cut edge pit-like corrosion indication on Type 409 showed a depth of corrosion of about 700 µm. Again, a deeper indication on the cut edge relative to the face surface is consistent with corrosion initiating on the cut edge and the need for the pit-like indications to initiate underneath a rust deposit during this exposure.

SUMMARY

The chromized surface layer formed on the IF steel substrate exhibits a lower pitting corrosion susceptibility as

Downloaded from http://meridian.allenpress.com/corrosion/article-pdf/75/11/1276/2655949/3319.pdf by guest on 03 October 2024

demonstrated by potentiodynamic polarization measurements. The lower susceptibility is related to the significantly elevated Cr content of the surface. Despite this, the chromized steel performed poorly in the ASTM B117 salt fog exposure due to the significant galvanic corrosion that occurred on the exposed cut edge. When corrected for the cut edge corrosion, chromized steel exhibited a mass loss comparable to the more highly alloyed Type 439 and Type 436 stainless steels, all of which being significantly lower relative to Type 409 and Type 409Al. Chromized steel and Type 409 were found to be prone to pit-like corrosion formed underneath rust deposits. The pit-like indication on the chromized steel surface tended to propagate laterally along the chromized surface layer/IF steel substrate interface rather than through the IF steel substrate interface.

ACKNOWLEDGMENTS

Financial support was provided by Natural Science and Engineering Council of Canada (NSERC) in the form of a Collaborative Research and Development (CRD) grant in partnership with Tenneco Automotive.

References

1. Y. Inoue, M. Kikuchi, "Present and Future Trends of Stainless Steel for Automotive Exhaust System," Nippon Steel Technical Report, no. 88, 2003, p. 62-69.
2. K. Żaba, M. Nowosielski, P. Kita, M. Kwiatkowski, T. Tokarski, S. Puchlerska, *Archives of Metallurgy and Materials* 60, 3 (2015): p. 1825-1831.
3. R. Baboian, "Designing Clad Metals for Corrosion Control," SAE Technical Paper 720514 (Evanston, IL: SAE, 1972).
4. C.S. Shepard , "Exhaust System Design-Art or Science?" SAE Technical Paper 690006 (Evanston, IL: SAE, 1969).
5. J.E. McDermot, A.G. Thomas, Z.M. Detweiler, "Methods for Chromium Coating," U.S. Patent US20190062856A1, 2019.
6. R.G.I. Leferink, H. Barten, W.M.M. Huijbregts, *VGB Kraftwerkstechnik* 73, 3 (1993): p. 269-275.
7. ASTM B117-16, "Standard Practice for Operating Salt Spray (Fog) Apparatus" (West Conshohoken, PA: ASTM International, 2018).
8. J.S. Kim, W.H.A. Peelen, K. Hemmes, R.C. Makkus, *Corros. Sci.* 44 (2002): p. 635-655.
9. T.J. Mesquita, E. Chauveau, M. Mantel, N. Kinsman, R.P. Nogueira, *Metall. Mater.* 66, 2 (2013): p. 173-178.
10. J. Shu, H. Bi, X. Li, Z. Xu, *Corros. Sci.* 57 (2012): p. 89-98.
11. M.I. Suleiman, I. Ragault, R.C. Newman, *Corros. Sci.* 36, 3 (1994): p. 479-486.

Downloaded from http://meridian.allenpress.com/corrosion/article-pdf/75/11/1276/2655949/3319.pdf by guest on 03 October 2024